Basic Physicochemical Properties of Polyethylene Glycol Coated Gold Nanoparticles Determine Their Interaction with Cells

Pablo del Pino [1,2,#,*], *Fang Yang* [3,#], *Beatriz Pelaz* [1,#], *Qian Zhang* [1], *Karsten Kantner* [1], *Raimo Hartmann* [1], *Natalia Martinez de Baroja* [2], *Marta Gallego* [2], *Marco Möller* [2], *Bella B. Manshian* [4], *Stefaan J. Soenen* [4], *René Riedel* [3], *Norbert Hampp* [3], *and Wolfgang J. Parak* [1,2,*],

[1]Fachbereich Physik, Philipps Universität Marburg, Marburg, Germany
[2]CIC biomaGUNE, San Sebastian, Spain
[3]Fachbereich Chemie, Philipps Universität Marburg, Marburg, Germany
[4]Radiology Department, KULeuven Campus Gasthuisberg, Leuven, Belgium
[#]authors contributed equally to this study
*corresponding authors: pdelpino@cicbiomagune.es, wolfgang.parak@physik.uni-marburg.de

ABSTRACT

A homologous nanoparticle library was synthesized in which gold nanoparticles were coated with polyethylene glycol, whereby the diameter of the gold cores, as well as the thickness of the shell of polyethylene glycol was varied. Basic physicochemical parameters of this two-dimensional nanoparticle library, such as size, ζ-potential, hydrophilicity, elasticity, and catalytic activity were determined. Cell uptake of selected nanoparticles with equal size yet varying thickness of the polymer shell, and their effect on basic structural and functional cell parameters was determined. Data suggests indicates that thinner, more hydrophilic coatings, combined with the partial functionalization with quaternary ammonium cations, result in a more efficient uptake, which relates to significant effects on structural and functional cell parameters.

The role of basic physicochemical parameters of the NPs towards their interaction with cells is still not fully unraveled.[2] The manifold final composition of the NPs makes it hard to define and measured in terms of physicochemical properties.[2] It even is complicated to synthesize a series of model NPs in which only one physicochemical property is varied, while the others are kept constant. Yet, some examples can be found in the literature, for instance, regarding size,[4] shape,[5] stiffness[6] or surface charge[7].

In the present study an array of NPs was synthesized, which takes into account the hybrid nature of NPs. Au NPs and polyethylene glycol (PEG) were used as main constituents of a series of PEGylated colloids, whereby the diameter of the inorganic Au cores d_C as well as the thickness of the PEG shell $1/2 \cdot d_S$ was varied, cf. Figure 1. In detail, differently sized citrate-capped Au NPs ($d_C \approx$ 14, 18, 23 and 28 nm[9]) were saturated with four different HS-PEG-COOH polymers with increasing molecular weight (ca. 1, 3, 5 and 10 kDa), thereby providing NPs with increasing shell thickness $1/2 \cdot d_S$. This in total provides an array of 4×4 = 16 samples in which each core was combined with each PEG, cf. the Supporting Information (SI). In this way, a size range d_{CS} from ca. 20 to 60 nm, widely used in cell studies (50 nm has been suggested as optimal for cell uptake[10]), was studied in detail.

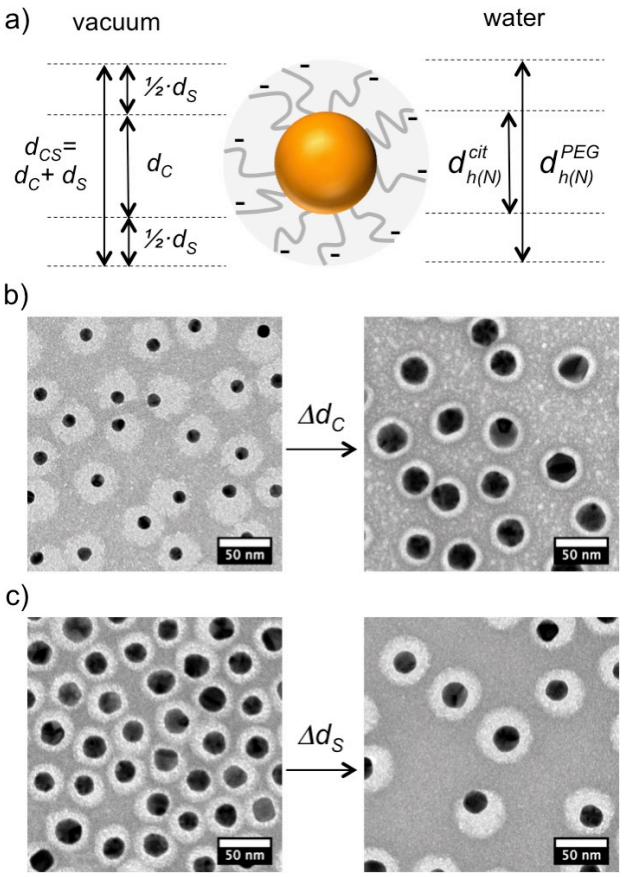

Figure 1. a) Scheme of PEGylated Au NPs, showing different properties in vacuum and in solution. d_C and d_{CS} refer to the diameters of the Au cores and of the cores with the PEG shell (the core-shell system), respectively, as determined by transmission electron microscopy (TEM). $d^{cit}_{h(N)}$ and $d^{PEG}_{h(N)}$ refer to the hydrodynamic diameters as obtained from the number distribution with dynamic light scattering (DLS) of the originally citric acid stabilized Au NPs before PEGylation and of the PEGylated NPs, respectively. b) Negative staining TEM micrographs of two types of PEGylated NPs are shown, in which d_C increases, while d_{CS} is kept constant at ca. 37 nm. c) Negative staining TEM micrographs of two types of PEGylated NPs are shown, in which d_{CS} increases while d_C is kept constant at ca. 23 nm. The scale bar is 50 nm.

A large set of basic physicochemical properties was determined for all NPs of the NP library. As measurements were carried out upon variation of two parameters (d_C and d_{CS}), dependencies in a two-dimensional parameter space can be systematically analyzed. This involves analysis of the NPs properties upon α) keeping the whole size d_{CS} of the NP constant ($\Delta d_{CS} = 0$), by increasing the size of the Au core ($\Delta d_C > 0$) and decreasing the thickness of the PEG shell ($\Delta d_S < 0$); β) simultaneously increasing the diameter of the NP core ($\Delta d_C > 0$) and the thickness of the PEG shell ($\Delta d_S > 0$); χ) keeping the core diameter constant ($\Delta d_C = 0$) and increasing the thickness of the PEG shell ($\Delta d_S > 0$); δ increasing the thickness of the PEG shell ($\Delta d_S > 0$) and reducing the core diameter ($\Delta d_C < 0$), cf. Figure 2a.

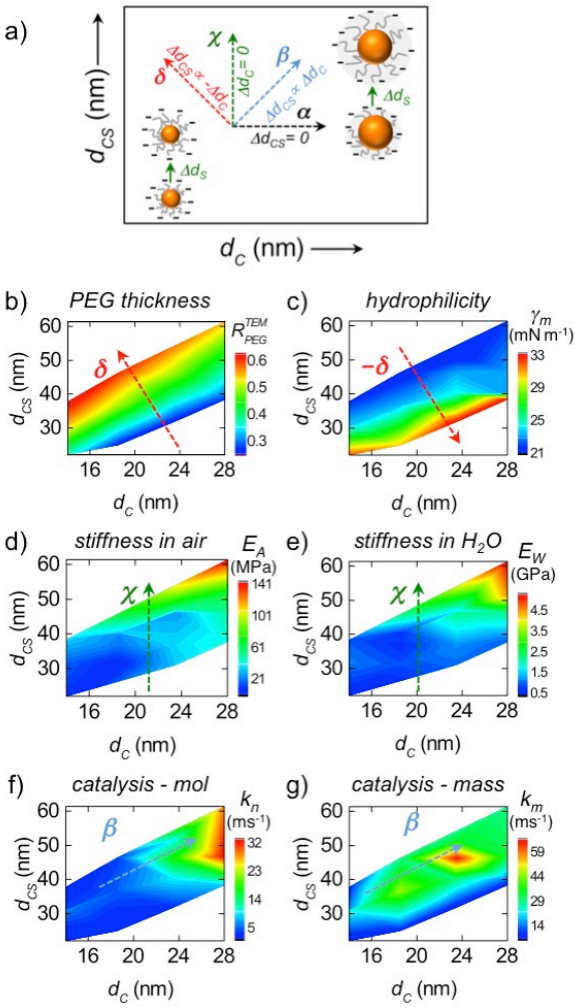

Figure 2. a) Diagram that schematically shows different variables related to the size of the PEGylated Au NPs;. b-g) Heatmaps of different physicochemical properties of the NPs in dependence of d_{CS} and d_C. The colour code refers to b) the proportion of PEG in the NP size R_{PEG}^{TEM}, c) the meso-equilibrium interfacial tension γ_m (i.e., hydrophilicity), d) the Young's modulus (modulus of elasticity) in air E_A, e) the Young's modulus in water E_W, f) the catalytic activity k_n at equal number of NPs, and g) the catalytic activity at equal mass of gold k_m. The parameters α, β, χ and δ are used to describe variations of d_C and/or d_S when $\Delta d_S = 0$, $\Delta d_{CS} \propto \Delta d_C$, $\Delta d_C = 0$ and $\Delta d_{CS} \propto -\Delta d_C$, respectively. In panel b-g) the dashed arrows point at the main variation in each case (i.e., δ, $-\delta$, χ or β).

The degree of PEGylation is expressed in terms of the parameter $R_{PEG}^{TEM} = \frac{\Delta d_S}{d_C + \Delta d_S}$, cf. Figure 2b. R_{PEG}^{TEM} equals 0 or 1 if the whole size (d_{CS}) comes from the Au core or the PEG shell, respectively. It is increased upon increasing the thickness of the PEG shell or by reducing the core diameter. As first parameter, the meso-equilibrium interfacial tension γ_m of the NPs is analyzed, cf. Figure 2c and SI. A high γ_m indicates a more hydrophilic NP surface, whereas a low γ_m ~~(< 36 mN·m^{-1})~~ indicates more hydrophobic NP surfaces.[11] γ_m almost does not depend on the size of the Au NP core, but strongly increases (i.e., hydrophilicity increases) upon decreasing the contribution of the amphiphilic PEG shell to d_{CS}, opposite to the increase in R_{PEG}^{TEM}. This indicates that surface tension and thus hydrophilicity of the Au NPs are influenced by the thickness of the PEG shell. The amphiphilic character of PEG motivates this a priori counterintuitive trend. Notice also that for the carboxylic-terminated PEGs used here, the higher the molecular weight, the smaller the ratio of ethylene glycol units to the carboxylic groups per NP results. The Young's modulus E of the NPs is only mildly affected upon variation of d_C (direction α) in the explored range, either in air (E_A) or water (E_W), cf. Figure 2d,e. A priori surprisingly, E increases upon increasing d_{CS} (direction χ). That is, thicker PEG coatings result in stiffer colloids. This can actually be explained by the high PEG packing density achieved, as deduced from the similar values of R_{PEG}^{TEM} and R_{PEG}^{DLS}, cf. SI. Notice that one could have expected smaller values of R_{PEG}^{TEM} (inferred from negative staining TEM, vacuum) than of R_{PEG}^{DLS} (inferred from DLS, water) due to hydration, however, they are very similar. Yet, for any of the samples studied, E_W values are significantly larger than the equivalent ones in air E_A (i.e., GPa *vs.* MPa), which suggests that water molecules stiffen inter-PEG interactions. This is actually in contradiction with a previous report about the mechanical properties of PEGylated surfaces.[12] Yet, PEG packing density plays a determining role with respect to the mechanical properties of PEGylated surfaces. E_W values obtained here

are in the same order of magnitude than E_W reported for viruses (ca. 0.12 – 2 GPa[13]) or those reported for BSA-coated Au NPs (*ca.* 1 – 2 GPa[14]), and clearly above those reported for natural vesicles or liposomes (ca. 0.01 – 0.1 GPa[15]).

Catalytic activity of the NPs was assayed towards their capability to trigger the reduction of methylene blue, cf. Figure 2f,g. Here results depend on the metrics. In case the same amount of Au NPs (ca. 0.2 nM) is used, catalytic activity scales with both the core size (d_C) and the core-shell size (d_{CS}), i.e., in direction β, cf. Figure 2f. At the same number of NPs, the NPs with bigger cores have a much higher surface area S_{NP} (i.e., $S_{NP} \propto d_C^2$), which typically will result in higher catalytic activity. On the other hand, in case the number of Au atoms (ca. 30 mg·L^{-1}) is kept constant (cf. Figure 2g), for smaller cores there are more NPs in solution as compared to NPs with bigger d_C (i.e., Au per NP $\propto d_C^3$). For this reason one would expect increase of surface reactivity should scale anti-proportional to d_C, as for smaller cores there are more NPs in solution. While this was found to be true for medium to big sized Au NPs (d_C from 24 - 28 nm at $d_{CS} \approx 45$ nm), for smaller NPs (d_C from 14 - 24 nm at $d_{CS} \approx 45$ nm) the opposite behavior is observed. We speculate that this is due to the presence of the PEG shell. Along the direction α the relative contribution of the PEG shell decrease. Very small cores are coated by a very thick shell of PEG, which may hinder diffusion of the methylene blue to the NP surface, and thus the thicker the PEG shell and the smaller the Au cores, the lower the catalytic activity.

In a next step we wanted to investigate the effect of these NPs on basic cellular parameters. From the 16 samples evaluated, we choose 4 samples with a fixed overall diameter $d_{CS} \approx 38$ nm, from "small" Au cores with thick PEG shell towards "big" Au cores with thin PEG shell. Thus, in the present study 4 samples with ca. equal d_{CS} and E_W, but varying γ_m and catalytic activity (k), were selected. As for observing NP uptake with fluorescence microscopy, terminal carboxylic groups

of the PEGs at the NP surface were partially covalently cross-linked with an amino-modified NIR dye (dyomics dy647P1) via EDC (1-Ethyl-3-(3-dimethylaminopropyl)carbodiimide) chemistry, cf. Figure 3a. Also, as internalization of NPs by cells highly depends on charge,[7] optionally, a quaternary ammonium group (2-aminoethyl trimethylammonium chloride hydrochloride, positive in all of the pH range) was also covalently attached to the surface of the NPs. In this way 2 sets of 4 different fluorescence labeled Au NPs, in which the overall NP diameter $d_{CS} \approx 38$ nm was kept constant, but the proportion of PEGylation was reduced in direction α, cf. Figure 3b. First, ζ-potential measurements in water as shown in Figure 3c demonstrate that attachment of a fluorescence label and optionally, quaternary ammonium groups, can modify the surface properties of NPs by partially neutralizing the net negatively charge of the NPs.

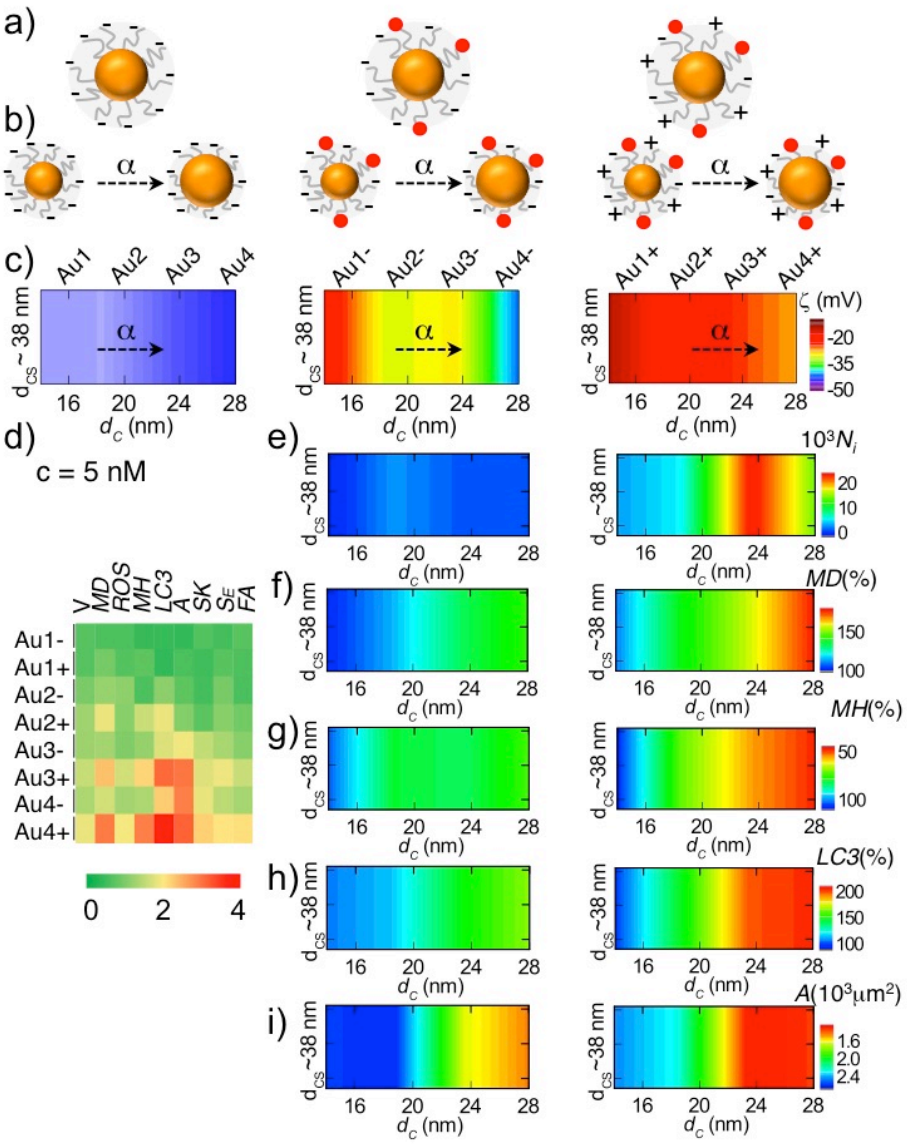

Figure 3. a) Schematic representation of the NP geometry: bare (left) and fluorescence-labeled (middle, right) PEGylated NPs. In the case of the NPs shown on the right, additional quaternary ammonium groups (+) were coupled to some of the negatively charged carboxyl termini (-) of the PEG molecules. b) For each type of NP a series of 4 samples with the same NP size d_{CS}, but variable core diameter (Au1, Au2, Au3, Au4) and thickness of the PEG shell along direction α was prepared. c) ζ-potential heatmaps for Au1 to Au4 (left), Au1- to Au4- (middle), and Au1+ to Au4+ (right), respectively. d) Heatmaps for various reporters related to structural and functional

cell parameters (i.e., *V*: viability; *MD*: membrane damage; *ROS*: production of reactive oxidative species; *MH*: mitochondrial health; *LC3*: autophagy; *A*: cell area; *SK*: cell skewness; S_E: endosomal size; *FA*: focal adhesion) for the NPs given at equal number (5 nM) to C17.2 cells, where Au1, Au2, Au3 and Au4 represent Au NPs with ca. the same d_{CS} (≈ 38 nm) yet PEGylated with ca. 10, 5, 3 and 1 kDa HS-PEG-COOH, respectively; the signs – and + stand for without and with addition of quaternary ammonium groups, respectively. e) Heatmaps for NPs internalized per cell (N_i). f-i) Heatmaps for selected parameters, i.e., more affected *MD*, *MD*, *LC3* and *A*, related to basic cellular parameters for the NPs given to C17.2 cells, for the fluorescence labeled NPs without (middle column) and with addition of quaternary ammonium groups (right column).

The two series of fluorescently labeled NPs (2×4 samples) were incubated with two cell lines, murine C17.2 neural progenitor and primary human umbilical vein endothelial cells (HUVECs). Following previously described protocols,[18] the following cellular parameters were analyzed: autophagy (*LC3*), cell area (*A*), endosome size (S_E), membrane damage (*MD*), mitochondrial health (*MH*), reactive oxidative species (*ROS*), cell skewness (*SK*), cell viability (*V*) and focal adhesion (*FA*). For cellular exposure studies, cells were incubated with the NPs at an equal number of NPs (1.25, 2.5, or 5 nM) or at equal mass of gold (62.5, 125, or 250 µg/mL; cf. SI). The NP uptake (N_i) was determined by ICP-MS . First, the NPs with the added quaternary ammonium groups were incorporated by cells to a higher extend than the negatively more charged ones, cf., Figure 3e,i. As demonstrated in Figure 3e upon exposing cells to the same number of NPs, with the same overall diameter d_{CS} but different contribution of the PEG shell, NP uptake differs along direction α. Uptake seems to be correlated with the presence of

quaternary ammonium groups, as in every case the presence of this group significantly enhances NP uptake. Interestingly, uptake is not directly related to the ζ-potential, as can be observed by comparing the middle and right panels in Figure 3c and 3e, i.e., samples with the same ζ-potential present quite different uptakes (e.g., $d_C \approx 16$ in the middle panel compared to $d_C \approx 24$ in the right panel). NP uptake does not seem to directly depend on only one of the physicochemical parameters studied here, cf. Figure 2. One could speculate that hydrophilicity (cf., γ_m along α at $d_{CS} \approx 38$ in Figure 2c) plays a role on NP uptake, however, quaternary ammonium non-coupled and coupled equivalent colloids present very different NP uptake profiles, although γ_m is only mildly affected by functionalization with the dye and the quaternary ammonium group (cf. SI, for comparison of γ_m for Au3- and Au3+, the most internalized species). The impact of PEGylation along direction χ on NP uptake has been already investigated in previous work [17], which concluded that NP uptake decreases in the direction χ due to the molecular weight of the PEG. Here in the direction α, we do not observe a linear trend with respect to the length of the PEG. Clearly, the architecture used in each case as a profound impact on the results, which illustrates how challenging is to draw general conclusions, even when comparing a model system such PEGylated NPs. We can conclude that the combination of more hydrophilic and partial coupling of quaternary ammonium groups results in a more efficient NP uptake, probably due to the interaction with negatively charged heparan proteoglycan sulfate receptors on the cell membrane[19].

The data with regard to cell function and structural parameters are intimately related to NP uptake. That is, when NPs are given at equal number of NPs, more NP uptake has a clear negative effect on membrane damage (cf. Figure 2f), mitochondrial health (cf. Figure 2g), autophagy (cf. Figure 2h) and cell area (cf. Figure 2h), whereas the other parameters are less

affected compared to the control cells, cf., Figure 3d. Gene expression (for a total of 84 genes involved in cytoskeletal signaling and regulation) results for C17.2 cells also indicate highest levels of upregulation in more internalized NPs, indicating clear alterations in cytoskeletal architecture and regulation, which is in line with the imaging results, cf. SI.

The same cell study was also carried out with HUVEC cells, yielding similar results. Likewise, when cells (either C17.2 or HUVEC) were incubated with NPs at equal mass of gold similar trends were found (cf. SI), although in general cells were less and slightly differently affected (e.g., viability is more affected), probably due to less NP uptake. Notice that, however, in case of equal mass of gold, NPs with smaller d_C (direction α) were more efficiently internalized. This is due to the metrics, i.e., a concentration of 250 μg/mL correspond to a relative number of NPs of ca. 8.5 : 3.5 : 1.7 : 1, with diameter of ca. 14, 18, 23 and 28 nm, respectively. Nevertheless, even though more "small" NPs were added and thereby were more internalized, the amount of gold found in the cells (mass of gold per cell) was bigger for the "bigger" NPs, which however did not negatively affect the cells.

The fundamental problem in correlating the interaction of PEGylated NPs with cells with their physicochemical properties is that many basic physicochemical parameters of the NPs, such as size, ζ potential, hydrophilicity, elasticity, and catalytic activity depend on the "type" of PEGylated Au NP, cf. Figure 2. In order to account for changes in size, which may be as well due to differences in core diameter as in thickness of the PEG shell, a 2-dimensional array of NPs had been synthesized in this work. In contrast to previous studies found in literature in the present work thus a homologous NP library had been created, in which not only one parameter (i.e. one dimension), but two parameters (i.e. two dimensions) had been varied. Analysis of the

dependence of physicochemical properties of the NPs due to PEGylation as shown in Figure 2 suggests, that hydrophilicity (as quantified here in terms of γ_m) is the parameter most directly influenced by PEGylation. R_{PEG}^{TEM} and γ_m increase in opposite directions as indicated in Figure 2a. In contrast to other NP libraries [21] PEGylation does not largely influence NP elasticity (E_A and E_W) and catalytic activity (k_n), where only thick PEG shells may reduce diffusion of reagents to the NP core.

Concerning interaction with cells, in previous work we had investigated the effect of the thickness of the PEG shell with the NP core size kept constant, i.e. variation in direction χ[17]. In the present work we focused on variation in direction α, i.e. variation of the PEG shell contribution upon keeping the total NP diameter constant. In direction α, γ_m clearly increases, cf. Figure 2c, i.e., reduction in PEGylation (R_{PEG}^{TEM} decreases in direction α) makes NPs more hydrophilic. PEG on the other hand is amphiphilic, that is, soluble in aqueous solution as in some less polar solvents such as chloroform. More hydrophilic NPs are incorporated best by cells, cf. Figures 2c and 3e, yet not in a linear fashion. Comparing Figures 3c and 3e suggests that the presence of quaternary ammonium groups combined with hydrophilicity is the more direct parameter, as changes in ζ potential (Figure 3c) are not directly translated into changes in NP internalization (Figure 3e). Note that we are referring here to the number of the incorporated NPs (Figure 3e), which forms a different metrics than the volume of incorporated NPs (Figure 3i). Reduction of cellular function and structure goes directly hand-in-hand with increased uptake of NPs (cf. Figures 3f,g,h with Figure 3e). While PEGylation can have some effect on catalytic activities of NPs, the data from Figures 2, f, g and Figures 3e,i rather suggest that reduction in

cellular function and structure of cells is not directly an effect of changes of catalytic activity upon PEGylation, but rather due to changes of the amount of incorporated NPs.

In summary the data obtained in this study indicate that PEGylated Au NPs may be designed to present many different physicochemical properties ("faces") and thus interact differently with cells, even when keeping the size d_{CS} constant. Effects of NPs on cellular function and structure for these NPs mainly scale with the amount of incorporated NPs, highly dependent on both partial functionalization with quaternary ammonium groups and the thickness of the PEG shell (lower for NPs with "thick" PEG coatings).

Acknowledgements:
Parts of this work were supported by the European Commission (project FutureNanoNeeds, grant to WJP), and by the MINECO (project MAT2013-48169-R to WJP and PdP). BP acknowledges a postdoctoral fellowship from the Alexander von Humboldt Foundation. QZ acknowledges a graduate student fellowship for the Chinese Scholarship Council (CSC). SJS is a post-doctoral fellow from the FWO Vlaanderen. BBM acknowledges the FWO Vlaanderen (Krediet aan Navorsers 1514716N).

Keywords: PEG • gold nanoparticles • physicochemical properties • toxicity • nanoparticle uptake

[1] P. Nativo, I. A. Prior, M. Brust, *ACS Nano* **2008**, *2*, 1639.
[2] P. Rivera Gil, D. Jimenez de Aberasturi, V. Wulf, B. Pelaz, P. del Pino, Y. Zhao, J. de la Fuente, I. Ruiz de Larramendi, T. Rojo, X.-J. Liang, W. J. Parak, *Acc. Chem. Res.* **2013**, *46*, 743.
[3] a) B. Pelaz, G. Charron, C. Pfeiffer, Y. Zhao, J. M. d. l. Fuente, X.-J. Liang, W. J. Parak, P. d. Pino, *Small* **2013**, *9*, 1573; b) P. M. Kelly, C. Aberg, E. Polo, A. O'Connell, J. Cookman, J. Fallon, Z. Krpetic, K. A. Dawson, *Nat. Nanotechnol.* **2015**, *10*, 472.
[4] K. Li, M. Schneider, *J Biomed Opt* **2014**, *19*, 101505.
[5] B. D. Chithrani, W. C. W. Chan, *Nano Lett.* **2007**, *7*, 1542.
[6] L. Zhang, Z. Cao, Y. Li, J.-R. Ella-Menye, T. Bai, S. Jiang, *ACS Nano* **2012**, *6*, 6681.
[7] D. Hühn, K. Kantner, C. Geidel, S. Brandholt, I. De Cock, S. J. H. Soenen, P. Rivera Gil, J.-M. Montenegro, K. Braeckmans, K. Müllen, G. U. Nienhaus , M. Klapper, W. J. Parak, *ACS Nano* **2013**, *7*, 3253.
[8] W. S. Cho, M. Cho, J. Jeong, M. Choi, B. S. Han, H. S. Shin, J. Hong, B. H. Chung, J. Jeong, M. H. Cho, *Toxicol Appl Pharmacol* **2010**, *245*, 116.
[9] N. G. Bastus, J. Comenge, V. Puntes, *Langmuir* **2011**, *27*, 11098.

[10] B. D. Chithrani, A. A. Ghazan, C. W. Chan, *Nano Lett.* **2006**, *6*, 662.
[11] S. Rana, X. Yu, D. Patra, D. F. Moyano, O. R. Miranda, I. Hussain, V. M. Rotello, *Langmuir* **2012**, *28*, 2023.
[12] X. Wang, R. N. Sanderson, R. Ragan, *The Journal of Physical Chemistry C* **2014**, *118*, 29301.
[13] M. G. Mateu, *Virus Res.* **2012**, *168*, 1.
[14] H. P. Wampler, A. Ivanisevic, *Micron* **2009**, *40*, 444.
[15] A. Calo, D. Reguera, G. Oncins, M.-A. Persuy, G. Sanz, S. Lobasso, A. Corcelli, E. Pajot-Augy, G. Gomila, *Nanoscale* **2014**, *6*, 2275.
[16] B. Hvolbæk, T. V. W. Janssens, B. S. Clausen, H. Falsig, C. H. Christensen, J. K. Nørskov, *Nano Today* **2007**, *2*, 14.
[17] B. Pelaz, P. Del Pino, P. Maffre, R. Hartmann, M. Gallego, S. Rivera-Fernandez, J. M. de la Fuente, G. U. Nienhaus, W. J. Parak, *ACS Nano* **2015**, *9*, 6996.
[18] a) B. B. Manshian, D. F. Moyano, N. Corthout, S. Munck, U. Himmelreich, V. M. Rotello, S. J. Soenen, *Biomaterials* **2014**, *35*, 9941; b) B. B. Manshian, S. Munck, P. Agostinis, U. Himmelreich, S. J. Soenen, *Scientific Reports* **2015**, *5*, 13890.
[19] H.-B. Pang, G. B. Braun, E. Ruoslahti, *Science Advances* **2015**, *1*.
[20] R. Hong, N. O. Fischer, T. Emrick, V. M. Rotello, *Chem. Mater.* **2005**, *17*, 4617.
[21] R. Hartmann, M. Weidenbach, M. Neubauer, A. Fery, W. J. Parak, *Angew. Chem. Int. Ed.* **2015**, *54*, 1365.

Text for Table of Contents

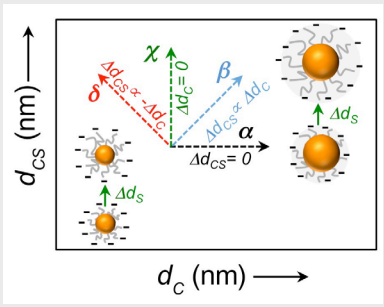

Pablo del Pino, Fang Yang, Beatriz Pelaz, Qian Zhang, Karsten Kantner, Raimo Hartmann, Natalia Martinez de Baroja, Marta Gallego, Marco Möller, Bella B. Manshian, Stefaan J. Soenen, René Riedel, Norbert Hampp, Wolfgang J. Parak**

Page No. – Page No.

How the Toxicity of Polyethylene Glycol Coated Gold Nanoparticles Depends on Basic Physicochemical Parameters—to be changed

1